Available online at www.sciencedirect.com
SCIENCE DIRECT®
Engineering Geology 69 (2003) 99–108
ENGINEERING GEOLOGY
www.elsevier.com/locate/enggeo

Parameterization of soil properties for a model of topographic controls on shallow landsliding: application to Rio de Janeiro

Renato Fontes Guimarães[a,*], David R. Montgomery[b,1], Harvey M. Greenberg[b,1], Nelson Ferreira Fernandes[c,2], Roberto Arnaldo Trancoso Gomes[c,2], Osmar Abílio de Carvalho Júnior[d,3]

[a] *Departamento de Geografia, Universidade de Brasília, Brasilia 70910-900, Brazil*
[b] *Earth and Space Sciences, University of Washington, Seattle, WA, USA*
[c] *Departamento de Geografia, Universidade Federal do Rio de Janeiro, Brazil*
[d] *Instituto Nacional de Pesquisas Espaciais (INPE), Brazil*

Received 16 April 2002; accepted 5 November 2002

Abstract

A key problem in the use of physically based models of landslide hazards is how to parameterize the representation of soil properties. We applied a physically based model for the topographic control on shallow landsliding (SHALSTAB) to two catchments in Rio de Janeiro to investigate the accuracy of model results in relation to parameterization of soil properties. In so doing, we address the relevance of values derived from laboratory tests to the field problem, as well as the trade-offs inherent in model parameterization. We ran the model for all combinations of reasonable cohesion, bulk density, and friction angle values and compared model predictions to mapped landslides scars. We rank sorted model performance through the proportion of the total area of landslide scars correctly predicted as potentially unstable. Application of the model to an area where soil properties are not well known can be based on either a standard parameterization that emphasizes topographic controls, or on local calibration of soil parameters against a map of known landslide locations. Our analysis suggests that, in general, acquisition of high-quality digital elevation models (DEMs) is more important than generation of spatially detailed soil property values for reconnaissance level assessment of shallow landslide hazards.

Keywords: Landslides; Model testing; Parameterization; Topographic; DEM

1. Introduction

Advances in spatially distributed modeling of complex hydrological and geomorphic processes have fostered development of a wide range of GIS-driven approaches to landslide hazard assessment in Europe, Japan, and the United States (e.g., Neuland, 1976;

* Corresponding author. Fax: +55-61-272-1909.
E-mail addresses: renato@unb.br (R.F. Guimarães), dave@geology.washington.edu (D.R. Montgomery), hgreen@u.washington.edu (H.M. Greenberg), nelson@igeo.ufrj.br (N.F. Fernandes), beto@igeo.ufrj.br (R.A. Trancoso Gomes), osmarjr@solar.com.br (O.A. de Carvalho).
[1] Fax: +1-206-543-3836.
[2] Fax: +55-21-2598-9474.
[3] Fax: +55-12-3945-6449.

0013-7952/02/$ - see front matter © 2002 Published by Elsevier Science B.V.
doi:10.1016/S0013-7952(02)00263-6

Carrara et al., 1977, 1991; Okimura and Ichikawa, 1985; Dietrich et al., 1993; Montgomery and Dietrich, 1994; van Asch et al., 1993; Busoni et al., 1995; Wu and Sidle, 1995). Process-based models are increasingly central to erosion and landslide studies and hazard assessments because such models allow spatially explicit examination of the potential effects of changes in the governing hydrological and geomorphic processes. For this reason, a variety of models have been developed and applied in studies of erosional processes (e.g., Moore et al., 1988) to locate saturation zones (e.g., O'Loughlin, 1986) and evaluate areas of a landscape shaped by different geomorphological processes (e.g., Dietrich et al., 1993). Process-based models for shallow landslide hazard assessment based on coupling digital elevation models (DEMs) to hydrological and slope stability models allow delineation of areas at risk for shallow landsliding (e.g., Okimura and Ichikawa, 1985; Dietrich et al., 1993; van Asch et al., 1993; Montgomery and Dietrich, 1994). One such model has been used to predict areas subject to shallow landsliding in both urban and rural settings in temperate regions of the western United States (Dietrich et al., 1993, 1995, 2001; Montgomery and Dietrich, 1994; Montgomery et al., 1998, 2000, 2001) and in tropical Brazil (Guimarães et al., 1999; Fernandes et al., 2001).

A central issue in the application of such models is how to parameterize soil properties given limitations in the availability of field or laboratory measurements commensurate to the spatial density of data necessary to set representative values for a continuous grid. Although soil parameters incorporated into a model can be based on generalization of soil properties obtained in field surveys, there are scale issues involved in the translation of laboratory values to the field problem. Here we investigate using knowledge of landslide locations to evaluate the parameterization of soil properties in two basins in southeastern Brazil where previous work documented landslides that occurred after heavy summer rainstorms in February 1996 (GEORIO, 1996). The variety of land cover and wide range of slopes in the study basin, together with the numerous landslides that occurred in that storm, provide an excellent opportunity to test the application of this model in a tropical environment.

2. Model of topographic control on shallow landsliding

The model that we used, SHALSTAB, is based on coupling a hydrological model to a limit equilibrium slope stability model to calculate the critical steady-state rainfall necessary to trigger slope instability at any point in a landscape (Dietrich et al., 1993, 1995, 2001; Montgomery and Dietrich, 1994; Montgomery et al., 1998, 2001). The hydrological model assumes that flow infiltrates to a lower conductivity layer and follows topographically determined flow paths, allowing calculation of the spatial pattern of equilibrium soil saturation (O'Loughlin, 1986). Specifically, local wetness (W) is calculated as the ratio of the local flux at a given steady-state rainfall (Q) to the flux upon complete saturation of the soil profile:

$$W = (Qa)/(bT\sin\theta) \tag{1}$$

where a is the upslope contributing area (m^2), b is the contour length across which flow is accounted for (m), T is the soil transmissivity (m^2/day), and θ is the local ground slope (degrees). Adopting the simplifying assumption that the saturated conductivity does not vary with depth results in $W = h/z$ for $W \leq 1$ (Dietrich et al., 1995), where h is the thickness of the saturated soil above the impermeable layer and z is the total thickness of the soil.

Combining this hydrological model with the infinite slope stability model allows prediction of the critical ratio of the steady-state rainfall to the soil transmissivity required to cause slope instability (Q/T)$_c$:

$$(Q/T)_c = (b\sin\theta/a)(\rho_s/\rho_w)[1 - (\tan\theta/\tan\phi)] \tag{2}$$

for cohesionless soils where ρ_s is the saturated bulk density of the soil, g is the gravitational acceleration, ρ_w is the density of water, and ϕ is the friction angle of the soil (Montgomery and Dietrich, 1994). For cohesive soils, (Q/T)$_c$ is given by

$$(Q/T)_c = (b\sin\theta/a)[[C/\rho_w gz\cos^2\theta\tan\phi] + (\rho_s/\rho_w)[1 - (\tan\theta/\tan\phi)]] \tag{3}$$

where C is the net apparent cohesion attributable to soil cohesion and root reinforcement and z is the soil thickness (Montgomery et al., 1998).

There is no mechanism in this model for generating pore pressures greater than hydrostatic and thus values of W greater than 1.0 imply that excess water runs off as overland flow. Slopes that are stable even when saturated ($W = 1.0$) are interpreted to be unconditionally stable and to require excess pore pressures to generate slope instability. Similarly, slopes predicted to be unstable even when dry ($W = 0$) are considered

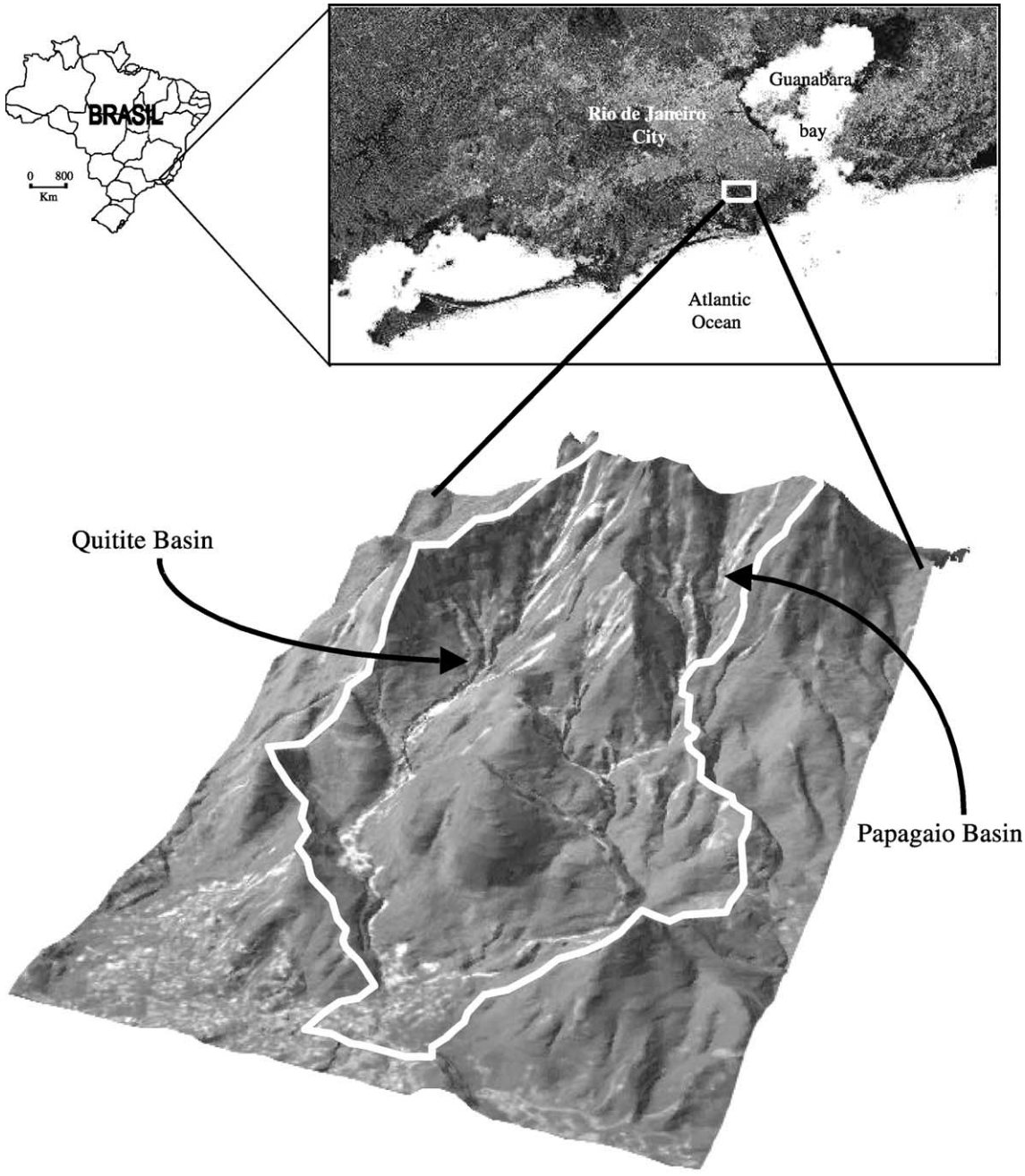

Fig. 1. Location map for the Quitite and Papagaio basins.

to be unconditionally unstable areas where soil accumulation would be difficult and, therefore, bedrock outcrops would be expected to occur. Critical rainfall values can be calculated for locations with slopes between these criteria, and these values can be used to identify areas with comparable topographic control on shallow landslide initiation.

The model components consist of topographic parameters (slope and contributing area), soil properties used in the slope stability model (friction angle, cohesion, depth, and bulk density), and hydrological factors (soil transmissivity and steady-state rainfall). The topographic parameters that determine the local water accumulation, which decreases the effective normal stress acting on hillslope materials, are set by the DEM quality and resolution. Soil properties can be treated either as spatially explicit when such information is available or as averaged properties generalized across a catchment or within soil types. Because the hydrological processes that drive landsliding vary over time, and rainstorm characteristics such as antecedent moisture, precipitation intensity, and duration all influence the magnitude of pore pressure response, the model seeks to provide a spatial index of relative hazard by combining the hydrological factors into a ratio that defines a relative stability index. SHALSTAB predicts the greatest potential for instability on steep slopes with large drainage areas (i.e., steep, wet areas). Based on Eq. (3), SHALSTAB classifies the landscape into categories of shallow landslide susceptibility defined as unconditionally stable ($\tan\theta \le \tan\phi[1-\rho_w/\rho_s]$), unconditionally unstable ($\tan\theta > \tan\phi$), and potentially unstable locations where relative landslide initiation hazard based on values of $(Q/T)_c$.

3. Study area

The study area consists of the Quitite and Papagaio basins in the neighborhood of Jacarepaguá in the western part of Rio de Janeiro, southeastern Brazil (Fig. 1). The 5.4-km^2 study area drains the western slope of the Massif of Tijuca and experienced numerous landslides triggered by an intense rainstorm in February 1996, during which 250 mm of precipitation fell in 48 h (Vieira et al., 1997). Coelho (1997) documented the dominance of shallow translational landslides developed at the soil–rock interface and exposures in landslide scars reveal that the slopes of the Quitite basin have soil thickness of 1–3 m. Aerial photographs of the study area taken about 2 months after the storm show hundreds of shallow landslides, debris flows, and debris avalanches. Human occupa-

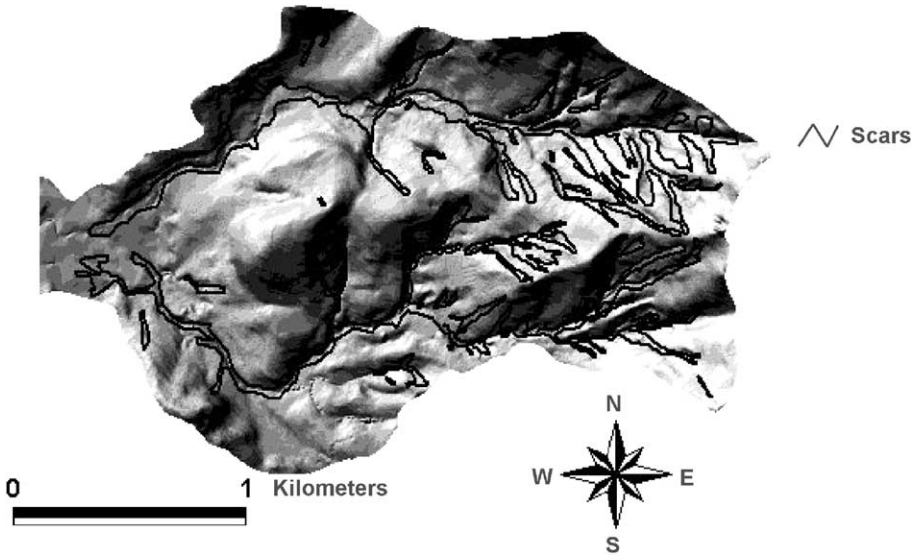

Fig. 2. Map of the landslide scars in the study area. Polygons represent landslide scars including landslide scarps, debris flow tracks, and deposits.

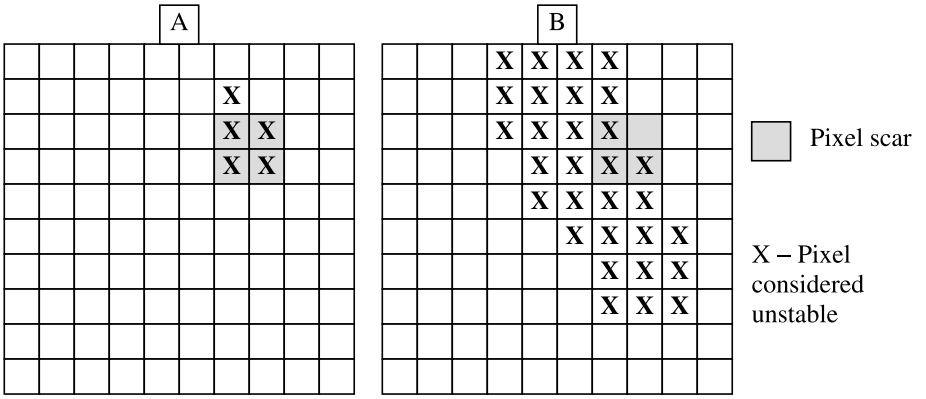

Fig. 3. Illustration of the method for determining the model fit index FI = PMS/PS. The two hypothetical cases illustrated here show examples where: (A) FI = 1.0, with all of the landslide scar pixels coincident with potentially unstable pixels and (B) FI = 0.75, where despite using the 30% of the potentially unstable pixels with the greatest potential for shallow landsliding, three quarters of the pixels covered by mapped landslide scars fall within potentially unstable pixels.

tion and use of the area are sparse and elevations range from 20 to 1000 m. Examination of 1:20,000 scale aerial photographs shows that native forest is the dominant vegetation in the basin headwaters, grassland dominates in other steep areas, and cleared forest dominates areas of gentle relief low in the catchments.

4. Methods

A 2-m grid DEM was created from digital contour coverage from a 1:10,000 scale topographic map and interpolated using the Topogrid module of ARC/INFO. Slope and contributing area values were ob-

For 5% of the database

Ranking positioning	Parameters Combination
1	**q2_45_15**
2	*q4_35_15*
3	q4 30 15

For 10% of the database

Ranking positioning	Parameters Combination
1	*q4_35_15*
2	**q2_45_15**
3	q4 30 15

For 20% of the database

Ranking positioning	Parameters Combination
1	q4_30_15
2	*q4_35_15*
3	**q2 45 15**

For 30% of the database

Ranking positioning	Parameters Combination
1	q4_30_25
2	*q4_35_15*
3	**q2 45 15**

Fig. 4. Relative rankings of parameter combinations using most hazardous 5%, 10%, 20%, and 30% of the total area of potentially unstable terrain. Note that the relative rankings for q4-35-15 and q2-45-15 vary depending upon the percentile of potentially hazardous terrain used for the comparison.

tained for the study area from the resulting DEM. Landslide scars were mapped from 1:20,000 scale aerial photographs to delineate polygons where landslides occurred (Fig. 2). A high-resolution photogrammetric enlarger was used to create a 1:10,000 scale map of landslide source areas, runout tracks, and deposits, which was then georeferenced to the high-resolution DEM.

A wide range of soil property values has been reported in adjacent basins with similar geological and geomorphological conditions. In laboratory tests, De Campos et al. (1992) found that ϕ varied between 28° and 44°, and that increased soil moisture reduced soil friction angles. Earlier work by Costa Nunes (1969) found that ϕ varied between 25° and 40° for soils from the Massif of Tijuca. In Nova Friburgo, (RJ), a nearby area with similar conditions, De Campos et al. (1997) adopted values of $\phi = 32.4°$ and $C = 1.5$ kPa as representative for saturated soil. De Ploey and Cruz (1979) carried out in situ field measurements in Caraguatatuba (SP) and found ϕ varied from 21° to 35° and ρ_s varied between 1.5 and 2.0 g/cm^3 for regolith developed on gneiss.

Using Eq. (3), we simulated the potential for shallow landsliding across the study area for the full range of potential parameter values reported in the literature. In order to reduce the number of possible parameter combinations and because we lack data on their spatial distribution, the soil cohesion and depth terms were combined into the ratio C/z. Hence, our analysis does not depend on specific values assumed for C or z. We used a suite of simulations for the full range of reported values of ϕ and ρ_s and a range of C/z values from 0 to 8 kPa m^{-1} to compare different simulations to the map of landslide scars. Establishing five different values for each soil parameter ($\phi = 25°$, 30°, 35°, 40°, and 45°; $\rho_s/\rho_w = 1.5$, 1.75, 2, 2.25, and 2.5; and $C/z = 0$, 2, 4, 6, and 8 kPa m^{-1}) resulted in 125 models for combinatory analysis. A routine in ARC macro language (AML) automated making shallow landslide hazard maps for each parameter combination.

4.1. Determination of the best-fit model

Naturally, an optimal model would predict 100% correspondence between mapped landslides and potentially unstable ground. But if a model considers a large proportion of an area unstable, and yet landsliding is restricted to a small portion of the terrain, then the interpretation of model effectiveness centers on the somewhat subjective assessment of the potential for future landsliding in areas identified as potentially unstable but which have not yet failed. In contrast, the correspondence between observed landslides and potentially unstable ground can be used to assess model performance more directly, as land-

Table 1
Ranking of the parameter combinations due to prediction performance where FOP is the final order positioning (i.e., the arithmetic mean of the rank ordering for the four percentile analyses discussed in the text)

FOP	C'/z	ϕ	ρ	FOP	C'/z	ϕ	ρ	FOP	C'/z	ϕ	ρ
1	2	45	1.5	35	1	40	2.25	69	0	40	1.5
2	1	45	1.75	36	2	35	1.5	70	2	30	2
3	4	30	1.5	37	4	25	1.75	71	4	25	2.5
4	4	35	1.5	38	4	30	2	72	2	30	2.25
5	2	40	1.75	39	8	25	2.5	73	0	35	2.5
6	4	40	1.75	40	2	45	2.25	74	0	35	2.25
7	2	40	1.5	41	4	35	2.25	75	0	35	2
8	4	25	1.5	42	8	30	2.5	76	0	35	1.75
9	0	45	2	43	0	40	2.25	77	2	30	2.5
10	1	45	1.5	44	2	35	2.25	78	0	35	1.5
11	4	35	1.75	45	4	45	2	79	1	30	1.5
12	2	45	1.75	46	1	45	2.5	80	1	30	1.75
13	4	30	1.75	47	2	40	2.25	81	2	25	1.5
14	4	40	1.5	48	2	40	2.5	82	1	30	2
15	4	40	2	49	0	40	2.5	83	1	30	2.25
16	4	45	1.5	50	1	40	1.5	84	1	30	2.5
17	0	45	1.75	51	0	40	2	85	2	25	1.75
18	4	45	2.25	52	1	40	2.5	86	2	25	2
19	2	40	2	53	4	35	2.5	87	2	25	2.25
20	1	40	2	54	0	45	1.5	88	0	30	2.5
21	1	45	2	55	0	45	2.5	89	0	30	2.25
22	2	45	2	56	4	25	2	90	0	30	1.75
23	2	45	2.5	57	4	30	2.25	91	0	30	2
24	4	35	2	58	2	35	2.5	92	0	30	1.5
25	4	40	2.25	59	0	40	1.75	93	2	25	2.5
26	4	45	2.5	60	1	35	2.25	94	1	25	1.5
27	4	45	1.75	61	1	35	1.75	95	1	25	1.75
28	0	45	2.25	62	1	35	2	96	1	25	2
29	1	40	1.75	63	1	35	2.5	97	1	25	2.25
30	4	40	2.5	64	4	30	2.5	98	1	25	2.5
31	1	45	2.25	65	2	30	1.5	99	0	25	2.25
32	2	35	1.75	66	4	25	2.25	100	0	25	2.5
33	2	35	2	67	2	30	1.75	101	0	25	2
34	8	25	2.25	68	1	35	1.5	102	0	25	1.75
								103	0	25	1.5

For rankings greater than 103, there are no areas predicted to be potentially unstable due to the combination of high-friction angle (ϕ) and high cohesion (C/z).

slides originating in areas predicted to be stable clearly constitute model failure. The total area predicted to be potentially unstable for each model run was set at the area occupied by the 5th, 10th, 20th, and 30th percentile of Q/T values for all potentially unstable ground identified for that model run (i.e., the associated percentage of the potentially unstable areas identified as at greatest risk of sliding). Thus, we do not pick a single value of Q/T to define unstable ground, rather we use specified proportions of the catchment area that defines the least stable ground to compare among the model runs. We define a model fit index (FI) as the proportion of area of landslide scars correctly predicted as potentially unstable. This index can be expressed as FI = PMS/PS, where PMS is the number of pixels that fall within both a landslide scar and areas predicted to be potentially unstable, and PS is the total number of pixels that fall within landslide scars. Fig. 3 shows two hypothetical examples of model performance where the location of landslides is compared to the 5% of the potentially unstable areas predicted to have the greatest potential for instability (Fig. 3A) and to the 30% of the potentially unstable areas predicted to have the greatest potential for instability (Fig. 3B). For each of the 125 models, we ran four percentile analyses (i.e., 5th, 10th, 20th, and 30th percentiles), resulting in 500 separate analyses.

As a shorthand for discriminating among model runs, we used a nomenclature where in the run labeled q0-25-15 the values of C/z, ϕ, and ρ_s/ρ_w correspond to 0, 25, and 1.5, respectively. Because a particular model run can provide the best prediction for the 5th percentile of the Q/T distribution for potentially unstable areas, but has a lower ranking for the 10th percentile analysis, we rank ordered the performance of each parameter combination based on the arithmetic mean for the four percentile runs (Fig. 4).

5. Results

Table 1 shows the final ranking related to different percentile averages. The grid based on $C/z = 2$ kPa, $\phi = 45°$, and $\rho_s/\rho_w = 1.5$ provided the best result among all possible combinations of soil parameters. In general, the best model parameterizations have high ϕ, modest to low C/z, and $1.5 < \rho_s/\rho_w < 1.75$, whereas

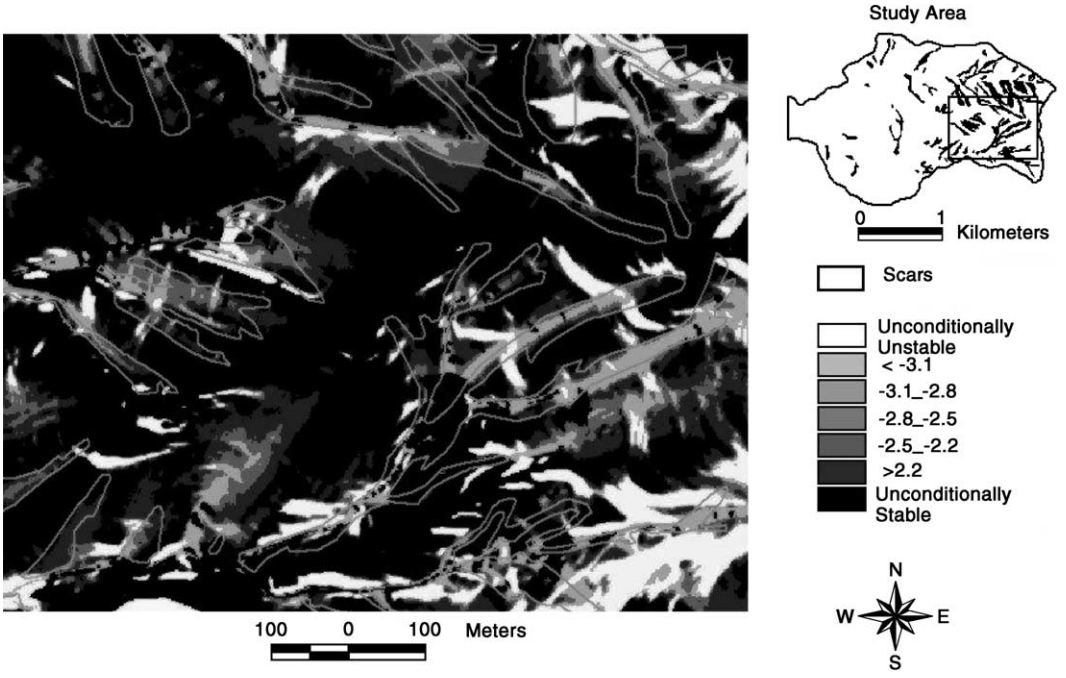

Fig. 5. Map of landslide scars overlaid on best-fit model results showing spatial coincidence between the unstable areas and scars.

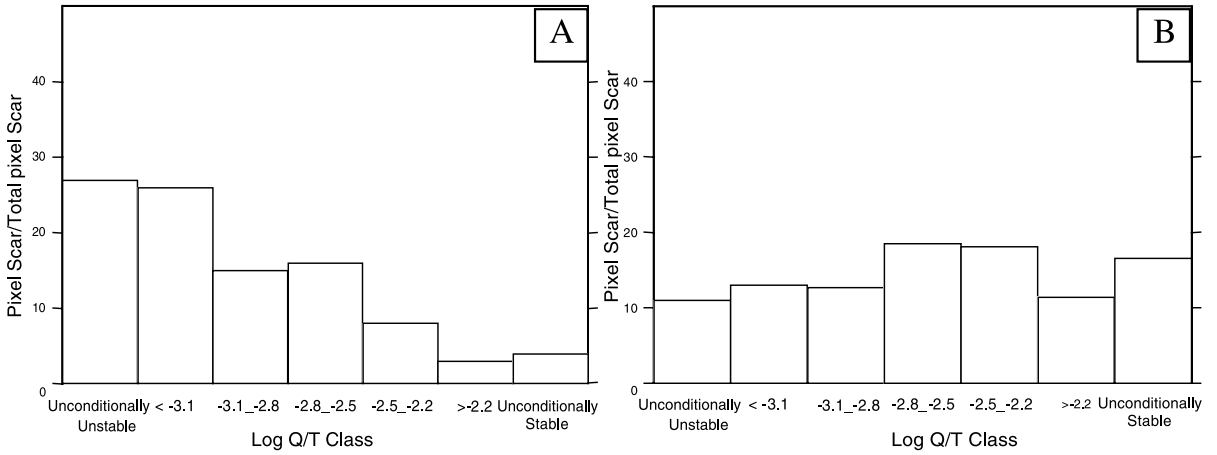

Fig. 6. Proportion of the total number of pixels in each log $(Q/T)_c$ class occupied by a mapped landslide for (A) the best-fit model and (B) the simple model.

parameterizations with low ϕ in combination with low C/z and $\rho_s/\rho_w>2$ resulted in poor model performance (Table 1).

Mapped landslide scars were overwhelmingly located in areas that the best-fit model predicted to be either unconditionally unstable, or potentially unstable (Fig. 5). We also verified that many unconditionally unstable areas are predominantly composed of bedrock outcrops.

The performance of the best model for the simple case of cohesionless soil (i.e., $C/z=0$) was compared to the overall best-fit model based on the frequency distributions of the ratio of the total number of landslide scar pixels to the total number of pixels in each relative instability classes (Fig. 6). In the best cohesionless model, 16% of all the scar pixels occurred in areas predicted to be unconditionally stable, in contrast to only 5% of the scar pixels in the best-fit model. In addition, each landslide was classified as associated with the minimum log $(Q/T)_c$ class within its boundary (Fig. 7). While a comparable numbers of landslides are associated with unconditionally unstable areas, the two models exhibit significant differences at higher log $(Q/T)_c$ values. In particular, in the best-fit model, 77 landslides occurred at the unconditionally unstable areas (Fig. 7A), in contrast to only

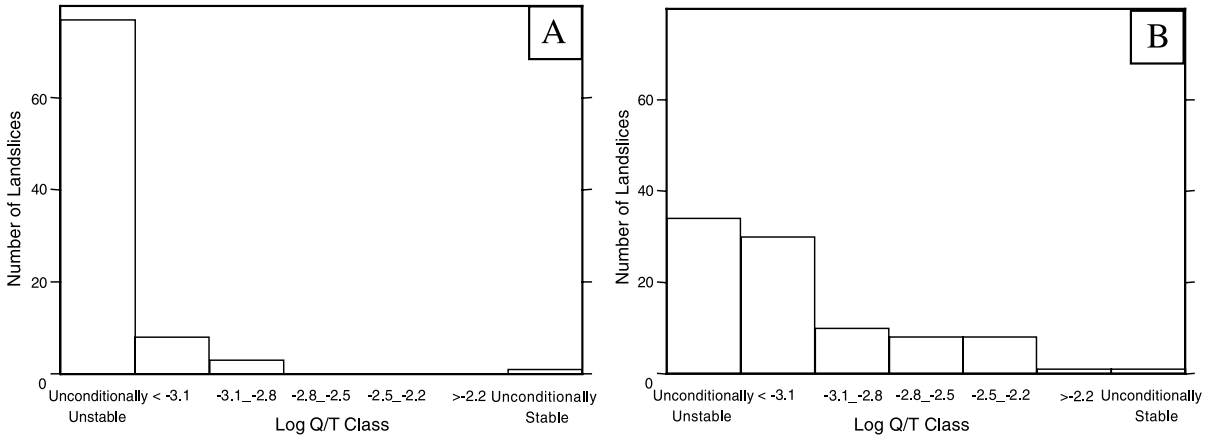

Fig. 7. Number of landslides associated with each log $(Q/T)_c$ class for (A) the best-fit model and (B) the simple model. Each landslide was assigned the minimum log $(Q/T)_c$ value within the border of the slide.

35 in the simple model (Fig. 7B). Although the best-fit model obtained better performance than the cohesionless model, the reasonable performance of even the simpler, cohesionless model in predicting landslide locations as relatively susceptible to failure indicates a strong topographic control on shallow landslide initiation in the Rio de Janeiro area.

6. Discussion and conclusions

In steep soil-mantled landscapes, landslides tend to occur in topographic hollows due to convergence of water and accumulation of colluvial soils that leads to a cycle of periodic filling and excavation by landsliding (Dietrich and Dunne, 1978). As the landscape evolves, such a cycle would be expected to reinforce the role of drainage area and slope as topographic controls on landsliding. But not all landslides are topographically driven. In the humid tropics, for example, one might expect thick regolith to mask topographic influences on landslide initiation. In our analysis of shallow landsliding in Rio de Janeiro, we find that parameter combinations emphasizing topographic control (through low C values) provide the best results.

Typically, little information is available to guide parameterization of soil properties in regional slope stability assessments. Significant information on spatial variability in soil properties related to slope stability is limited to rare case studies (e.g., Burton et al., 1998). Even though many workers adopt stochastic simulations for parameterizing soil properties in landslide hazard models, it remains unclear how to best translate soil properties determined in laboratory tests into representative values for landscape scale simulations—let alone how to distribute those values across the topography. The calibration of soil properties against a map of scars obtained from aerial photograph interpretation allows calibration of effective values for soil parameters in basin scale models such as SHALSTAB. Our analysis suggests that parameter values defined by calibration of modeling against scar locations can be used to extrapolate such simulations to similar areas for an initial analysis of potentially unstable ground.

Quantitative analysis of both the best-fit model and the simpler cohesionless model showed that shallow landslide initiation retains a strong topographic control in spite of the tropical soils. Moreover, the overall ranking of simulation performance showed that low values of friction angle yielded poor results, whereas variations in the soil density had little influence on model performance. Even though the model is very sensitive to the values of ϕ, C/z, and ρ_s/ρ_w—as all physically based landslide models—the best-fit model does not correspond to a parameterization with typical field values of soil properties. We suspect that this may reflect that friction angles are high in the low-confining stress environment of surficial soils, and that field scale cohesion is low due to scaling effects associated with translating the properties of laboratory samples to an entire landslide. Accurate portrayal of steep convergent terrain appears more important, and is certainly more attainable than spatially accurate characterization soil parameter values. Consequently, we suggest that greater effort and emphasis should be placed on acquisition of high-resolution, high-quality topographic data than on improved estimates of soil property values for use in mapping of relative landslide hazards.

References

Burton, A., Arkell, T.Jh., Bathurst, J.C., 1998. Field variability of landslide model parameters. Environmental Geology 35, 100–114.

Busoni, E., Sanchis, P.S., Calzolari, C., Romognoli, A., 1995. Mass movement and erosion hazard patterns by multivariate analysis of landscape integrated data: the upper Orcia river valley (Siena, Italy) case. Catena 25, 169–185.

Carrara, A., Pugliese Carratelli, E., Merenda, L., 1977. Computer-based bank and statistical analysis of slope instability phenomena. Zeitschrift fur Geomorphologie 21, 187–222.

Carrara, A., Cardinali, M., Detti, R., Guzzetti, F., Pasqui, V., Reichenback, P., 1991. GIS techniques and statistical models in evaluating landslide hazard. Earth Surface Processes and Landforms 16, 427–445.

Coelho, A.L., 1997. Geologia Estrutural e Hidrogeologia da Região do Quitite, Jacarepaguá (RJ): Condicionantes dos Escorregamentos nas Encostas. Monografia. Departamento de Geologia (UERJ) Rio de Janeiro. 29 pp.

Costa Nunes, A.J., 1969. Landslides in soils of decomposed rock due to intense rainstorms. VII Intern. Confer. on Soil Mech., Found. Eng., Mexico, 547–554.

De Campos, T.M.P., Andrade, M.H.N., Vargas Jr., E.A., 1992. Unsaturated colluvium over rock slide in a forest site in Rio de Janeiro. 6th International Symposium on Landslides, 1357–1364.

De Campos, T.M.P., Vargas Jr., E.A., Amaral, C.P., Dell Avanzi, E., 1997. Instabilization factors of the residual soil slope in Nova Friburgo, Rio de JaneiroII^{o} COBRAE, RJ, vol. 2, pp. 967–975.

De Ploey, J., Cruz, O., 1979. Landslides in the Serra do Mar, Brazil. Catena 6, 111–122.

Dietrich, W.E., Dunne, T., 1978. Sediment budget for a small catchment in mountainous terrain. Zeitschrift fur Geomorphologie. Supplementband 29, 191–206.

Dietrich, W.E., Wilson, C.J., Montgomery, D.R., McKean, J., 1993. Analysis of erosion thresholds, channel networks and landscape morphology using a digital terrain model. Journal of Geology 101, 259–278.

Dietrich, W.E., Reiss, R., Hsu, M.-L., Montgomery, D.R., 1995. A process-based model for colluvium soil depth and shallow landsliding using digital elevation data. Hydrological Process 9, 383–400.

Dietrich, W.E., Bellugi, D., Real de Asua, R., 2001. Validation of the shallow landslide model, SHALSTAB, for forest management. In: Wigmosta, M.S., Burges, S.J. (Eds.), Land Use and Watersheds: Human Influence on Hydrology and Geomorphology in Urban and Forest Areas. Water Science and Application Monograph, vol. 2. American Geophysical Union, pp. 195–227.

Fernandes, N., Guimarães, R., Gomes, R., Vieira, B., Montgomery, D., Greenberg, H., 2001. Geomorphological controls of landslides in Rio de Janeiro: field evidences and modeling. Transactions-Japanese Geomorphological Union 22 (4), C-67.

GEORIO, 1996. Estudos Geológicos-Geotécnicos a Montante dos Condomínios Capim Melado e Vilarejo, Jacarepaguá. Relatorio Tecnico, Rio de Janeiro (96 pp.).

Guimarães, R.F., Montgomery, D.R., Greenberg, H.M., Gomes, R.A.T., Fernandes, N.F., 1999. Application of a model for the topographic control on shallow landslides to catchments near Rio de Janeiro. IAMG99-Annual Conference of the International Association of Mathematical Geology, Trondheim, Noruega. vol. 1, pp. 349–354.

Montgomery, D.R., Dietrich, W.E., 1994. A physically-based model for the topographic control on shallow landsliding. Water Resources Research 30, 1153–1171.

Montgomery, D.R., Sullivan, K., Greenberg, M.H., 1998. Regional test of a model for shallow landsliding. Hydrological Processes 12, 943–955.

Montgomery, D.R., Schmidt, K.M., Greenberg, H.M., Dietrich, W.E., 2000. Forest clearing and regional landsliding. Geology 28, 311–314.

Montgomery, D.R., Greenberg, H.M., Laprade, B., Nasham, B., 2001. Sliding in Seattle: test of a model of shallow landsliding potential in an urban environment. In: Wigmosta, M.S., Burges, S.J. (Eds.), Land Use and Watersheds: Human Influence on Hydrology and Geomorphology in Urban and Forest Areas-Water Science and Application Monograph, vol. 2. American Geophysical Union, pp. 59–73.

Moore, I.D., O'Loughlin, E.M., Burch, G.J., 1988. A contour-based topographic model for hydrological and ecological applications. Earth Surface Processes and Landforms 13, 305–320.

Neuland, H., 1976. A prediction model of landslips. Catena 7, 205–221.

Okimura, T., Ichikawa, R., 1985. Prediction methods for surface failures by movements of infiltrated water in a surface soil layer. Natural Disaster Science 7, 41–51.

O'Loughlin, E.M., 1986. Prediction of surface saturation zones in natural catchments by topographic analysis. Water Resources Research 22, 794–804.

van Asch, T., Kuipers, B., van der Zanden, D.J., 1993. An information system for large scale quantitative hazard analyses of landslides. Zeitschrift fur Geomorphologie. Supplementband 87, 133–140.

Vieira, B.C., Vieira, A.C.F., Fernandes, N.F., Amaral, C.P., 1997. Estudo Comparativo dos Movimentos de Massa Ocorridos em Fevereiro de 1996 nas Bacias do Quitite e Papagaio (RJ): Uma Abordagem Geomorfológica. II Pan-American Symposium on Landslides/II Conferência Brasileira Sobre Estabilidade de Encostas, Rio de Janeiro, Brasil, vol. 1, pp. 165–174.

Wu, W., Sidle, R.C., 1995. A distributed slope stability model for steep forested basins. Water Resources Research 31, 2097–2110.